Organocatalytic Enantioselective Construction of Conformationally Stable C(sp2)–C(sp3) Atropisomers

(Article begins on next page)

22 July 2024

Organocatalytic Enantioselective Construction of Conformationally Stable $C(sp^2)$–$C(sp^3)$ Atropisomers

Giulio Bertuzzi,[a,†] Vasco Corti,[a,†] Joseph A. Izzo,[a] Sebastijan Ričko,[a,b] Nicolaj Inunnguaq Jessen[a] and Karl Anker Jørgensen*

[a] Department of Chemistry, Aarhus University, DK-8000 Aarhus C, Denmark

[b] Aarhus Institute of Advanced Studies (AIAS), Aarhus University, Høegh-Guldbergs Gade 6B, DK-8000 Aarhus C, Denmark

[†] G.B. and V.C. contributed equally to this work

ABSTRACT. Non-biaryl atropisomers are molecules defined by a stereogenic axis featuring at least one non-arene moiety. Among these, scaffolds bearing a conformationally stable $C(sp^2)$–$C(sp^3)$ stereogenic axis have been observed in natural compounds, however their enantioselective synthesis remains almost completely unexplored. Herein, we disclose a new class of chiral $C(sp^2)$–$C(sp^3)$ atropisomers obtained with high levels of stereoselectivity (up to 99% ee) by means of an organocatalytic asymmetric methodology. Multiple molecular motifs could be embedded in this class of $C(sp^2)$–$C(sp^3)$ atropisomers, showing a broad and general protocol. Experimental data provide strong evidence for the conformational stability of the $C(sp^2)$–$C(sp^3)$ stereogenic axis (up to $t_{1/2}^{25\,°C} > 1000$ y) in the obtained compounds and show kinetic control over this rare stereogenic element. This, coupled with DFT calculations, suggests that the observed stereoselectivity arises from a Curtin-Hammett scenario establishing an equilibrium of intermediates. Furthermore, experimental investigation led to the evidence for the operating principle of central-to-axial chirality conversions.

INTRODUCTION

Atropisomerism, the identifying property of molecules displaying restricted rotation around a σ-bond, can arguably be defined as a delicate and elusive type of stereoisomerism. Interconversion of atropisomers, depending on various conditions (temperature, hydrogen-bond interactions, light irradiation etc.), is relatively easy. *ortho*-Substituted (hetero)biaryls are a widespread and extensively studied class of atropisomeric molecules, for which a plethora of elegant

1

stereoselective synthetic methodologies are routinely being developed,[1-4] as they find application in catalysis,[5-7] drug discovery,[8,9] and material chemistry.[10,11] In contrast, atropisomerism in *non-biaryl* compounds is considerably underrepresented.[12-20] Consequently, methodologies directed towards their preparation are sporadic. Molecular frameworks exhibiting a conformationally stable $C(sp^2)$–$C(sp^3)$ stereogenic axis represent an example of this.

Interestingly, nature is capable of synthesizing $C(sp^2)$–$C(sp^3)$ atropisomers, as demonstrated by the isolation of natural products such as Pegaharmols A-B,[21] Cordypyridones A-B[22,23] (Figure 1a) and Bisnicalaterine A.[24] It should be noted that these compounds were isolated as atropisomeric-diastereomeric-mixtures, showing, in many cases, little or no control by nature of such a stereogenic element. The lack of selective formation of these compounds in nature, coupled with the very limited number of synthetic procedures, renders the stereoselective preparation of $C(sp^2)$–$C(sp^3)$ atropisomers tremendously alluring.

Archetypal synthetic scaffolds displaying restricted rotation around a $C(sp^2)$–$C(sp^3)$ single bond, among which only a few chiral compounds exist (Figure 1b), include: encumbered naphthyl dialkyl carbinols, 9-arylfluorenes, and aryltriptycenes. Many of these examples do not possess a center of asymmetry and are therefore achiral molecules that can be isolated as a pair of conformational diastereomers, due to the sole presence of a $C(sp^2)$–$C(sp^3)$ stereogenic axis.[25-28] Chiral $C(sp^2)$–$C(sp^3)$ atropisomers exhibiting axial chirality can be achieved if the axis displays a six-fold stereogenicity.[29-31] Recently, Sparr *et al.* disclosed an elegant methodology targeting the asymmetric preparation of aryltriptycenes in which either the antiperiplanar (*ap*) or the clinal (*c*) stereoisomers could be synthesized by careful selection of the ligand structure (Figure 1c).[29] Alternatively, the introduction of stereogenic centers results in the formation of chiral $C(sp^2)$–$C(sp^3)$ atropisomers. The stereoselective synthesis of such intriguing compounds has, according to our knowledge, not been achieved.
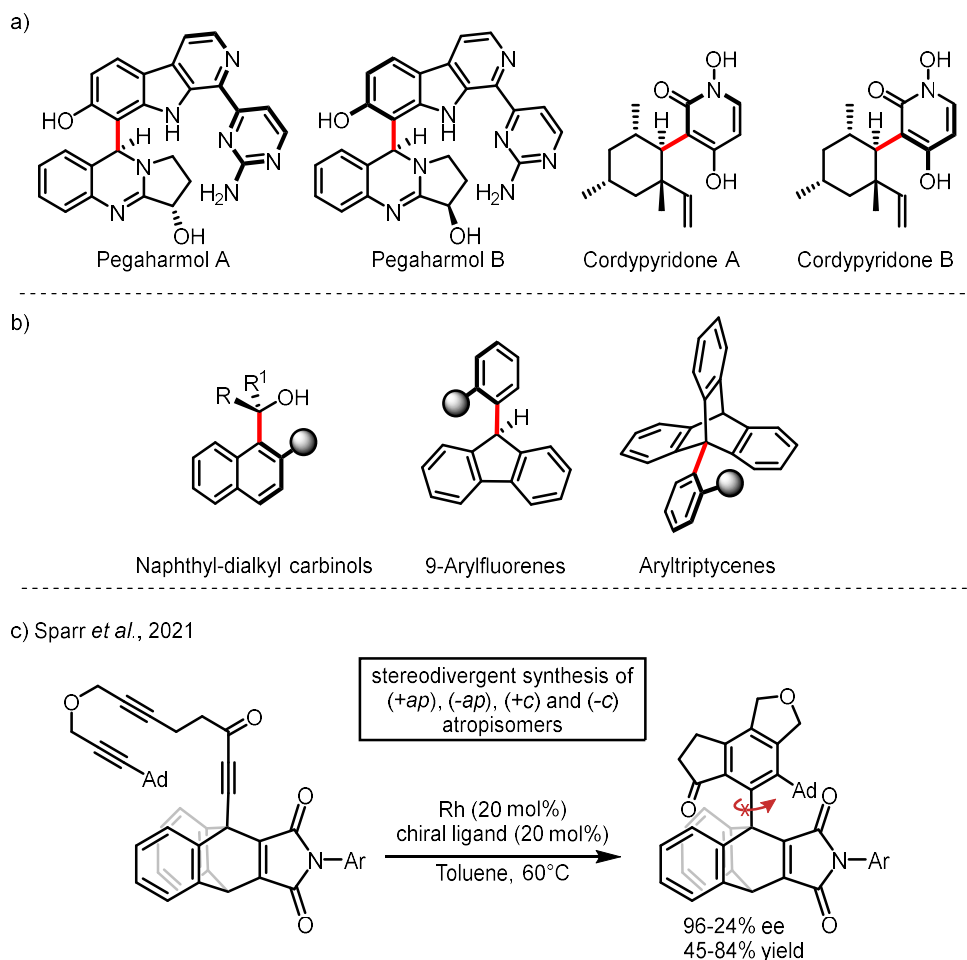
Figure 1. Natural and synthetic products featuring a C(sp²)–C(sp³) stereogenic axis. a) Naturally occurring compounds exhibiting C(sp²)–C(sp³) atropisomerism. b) Known molecular scaffolds having restricted rotation around a C(sp²)–C(sp³) bond. c) Stereodivergent synthesis of aryltriptycene derivatives featuring sixfold stereogenicity.

The presence of conformational diastereomers arising from a C(sp²)–C(sp³) stereogenic axis is observed or postulated in a number of reports dealing with *central-to-axial* chirality conversions. [32-36] In all cases, the rotational barrier around the C(sp²)–C(sp³) axis is low, preventing the two rotamers to be defined atropisomers. Moreover, a direct measurement of the rotational barrier and proof of any conformational stability is hardly achievable. For example, Rodriguez *et al.* observed 1,4-dihydropyridine derivatives as pair of conformational diastereoisomers in a 2.6:1 ratio (***ap*-DHPy** and ***sp*-DHPy** conformers, Scheme 1a) under dynamic equilibration. [33] Indeed, the authors measured, by dynamic NMR experiments, a rotational barrier of 13.4 kcal mol⁻¹ (corresponding to

a half-life time, $t_{1/2}$, <1 ms). Therefore, the characterization and the evaluation of the properties of each rotamer is not possible due to the impossibility of their isolation.

Scheme 1. a) Rapid equilibration of conformational diastereoisomers of 4-aryldihydropyridines. b) Asymmetric synthesis of conformational diastereomers under thermodynamic control. c) Identification of a new class of $C(sp^2)$–$C(sp^3)$ atropisomers and their stereoselective preparation.

a) Rodriguez *et al.*, 2016
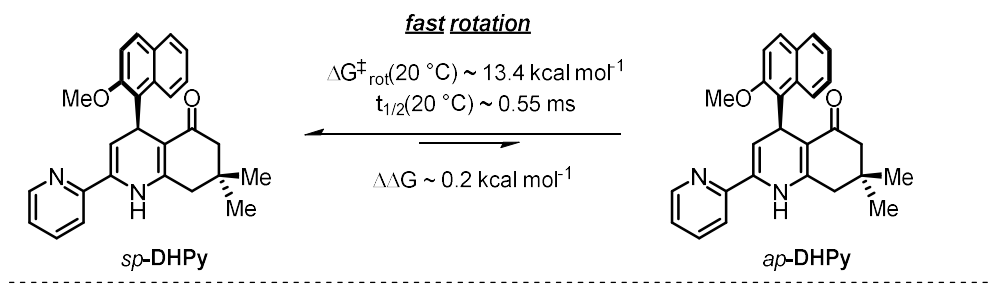
b) Bencivenni *et al.*, 2017
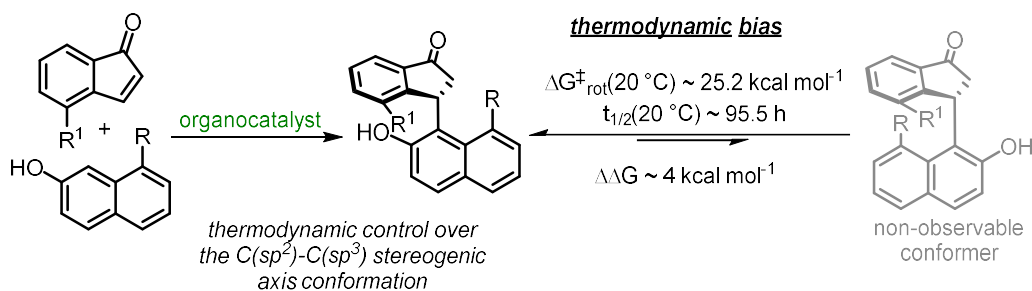
c) This work
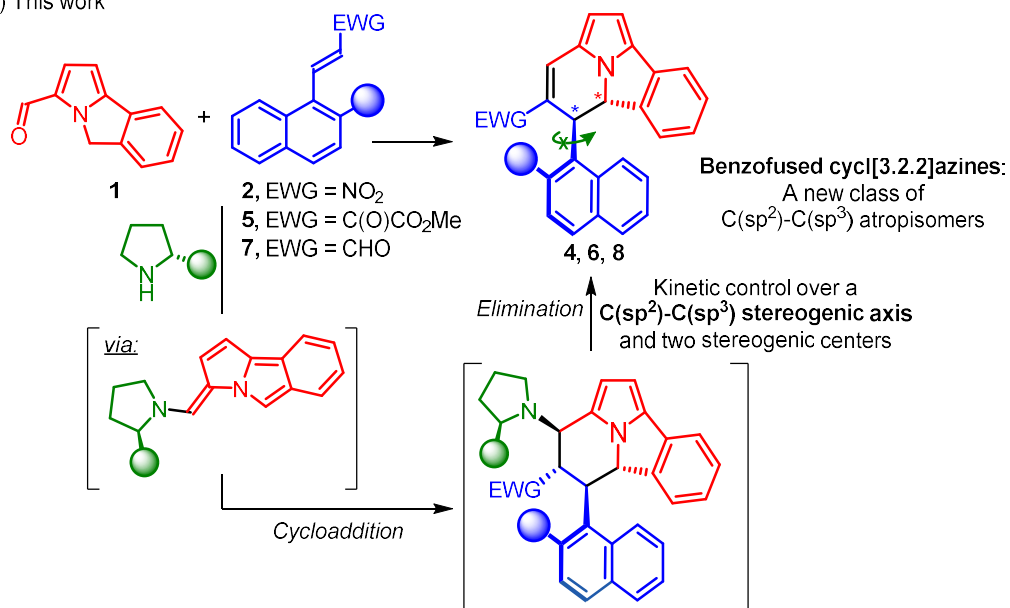
In order to achieve conformationally stable $C(sp^2)$–$C(sp^3)$ atropisomers, the reaction product needs to be designed to fulfill specific requirements: 1) The rotational barrier around the $C(sp^2)$–$C(sp^3)$ axis should be high enough to allow isolation, characterization, storage, and manipulation of the atropisomeric products, without any loss of the stereochemical information derived from the stereogenic axis (ΔG >30 kcal mol^{-1}).[37] This is a challenge because, in contrast to the congested planar environment of a common $C(sp^2)$–$C(sp^2)$ axis, the geometry of an sp^3-carbon allows for easier rotation in a conical 3D-space. 2) Generally, rotation around a stereogenic $C(sp^2)$–$C(sp^3)$ axis creates a pair of diastereomers, which differ in relative stability. The accessibility of both atropisomers is of the utmost importance to exclude thermodynamic control over the stereogenic axis and to measure the related properties. Thus, the product must not show an overwhelming thermodynamic preference for one of the two diastereomers.

The difficulty encountered in simultaneously fulfilling these arduous and constraining criteria renders the preparation of such molecules an unmet challenge. Therefore, devising an efficient stereoselective methodology can become a daunting task. An initial attempt was presented by Bencivenni *et al*. (Scheme 1b).[38] Unfortunately, the relative thermodynamic stability of the rotamers and the relatively low barrier of rotation prevented the authors from demonstrating the existence of conformational stability.

Our interest towards the preparation of optically active cyclazine moieties[39] prompted us to envision these architectures as an unexpected class of conformationally stable molecules exhibiting $C(sp^2)$–$C(sp^3)$ atropisomerism, thus expanding the borders of knowledge in the field of atropisomeric *non*-biaryls. Herein, we disclose an unprecedented example of a catalytic construction of a conformationally stable $C(sp^2)$–$C(sp^3)$ stereogenic axis under kinetic control (Scheme 1c). The reaction proceeds *via* an enantioselective aminocatalytic cycloaddition between 5*H*-benzo[*a*]pyrrolizine-3-carbaldehydes **1** and nitroolefins **2**, α,β-unsaturated ketoesters **5** or α,β-unsaturated aldehydes **7**. This affords optically active partially saturated cycl[3.2.2]azines **4**, **6** or **8** with a high degree of control over a $C(sp^2)$–$C(sp^3)$ stereogenic axis. This also represents the first access to atropisomeric cyclazine-cores.

RESULTS AND DISCUSSION

Reaction design and development. Our investigations started with the pyrrolidine/2-methylbenzoic acid **3a** co-catalyzed cycloadditions of **1a** with *ortho*-chloronitrostyrene **2a** or *ortho*-bromonitrostyrene **2b**, rendering compounds **4aa** and **4ab**, respectively (Figure 2, Top). Surprisingly, these cycloadducts were found to exist as a mixture of rotamers. Density-functional theory (DFT) calculations, performed on the system (*vide infra*), predicted the rotational barrier around the C5-aryl bond for **4aa** (23.8 kcal mol^{-1}; $t_{1/2}^{25\,°C}$ = 8.58 h) and **4ab** (25.9 kcal mol^{-1}; $t_{1/2}^{25\,°C}$ = 314 h). Rational design of a more synthetically useful product, with a longer half-life time, pointed to compound **4ac**, for which DFT calculations predicted a rotational barrier of 32.0 kcal mol^{-1} ($t_{1/2}^{25\,°C}$ = 1100 years and $t_{1/2}^{60\,°C}$ = 4.29 years). Moreover, the difference in energy between the two atropisomers was calculated to be low enough that both could be observed under thermodynamic equilibrium (0.92 kcal mol^{-1} corresponding to a 4.7:1 ratio at room temperature). Pyrrolidine/acid **3a** co-catalyzed cycloaddition between **1a** and nitroolefin **2c** smoothly afforded the desired product **4ac** as a single racemic C(sp^2)–C(sp^3) atropisomer. Heating compound **sp-4ac** at 130 °C for several hours resulted in the observation of its rotamer **ap-4ac** (Figure 2, Bottom) confirming that the C(sp^2)–C(sp^3) axis is a stable stereogenic element at room temperature. This also enables the experimental determination of the rotational barrier value connecting **sp-4ac** and **ap-4ac** (32.7 kcal mol^{-1}, see Supporting Information). After thermodynamic equilibration between **sp-4ac** and **ap-4ac** was reached, an experimental 2.5:1 ratio in favor of **sp-4ac** was obtained. This corresponds to a 0.73 kcal mol^{-1} difference in energy at 130 °C between the two atropisomers and to a rotational barrier connecting **ap-4ac** to **sp-4ac** of 30.9 kcal mol^{-1}. Thus, it can be affirmed that **ap-4ac** is a stable atropisomer at room temperature. Ultimately, it was also demonstrated that the reaction does not deliver the thermodynamic ratio of products, nor that it undergoes equilibration during the reaction course. These properties identify **4ac** as the optimal candidate for the development of a stereoselective methodology towards compounds exhibiting C(sp^2)–C(sp^3) atropisomerism.
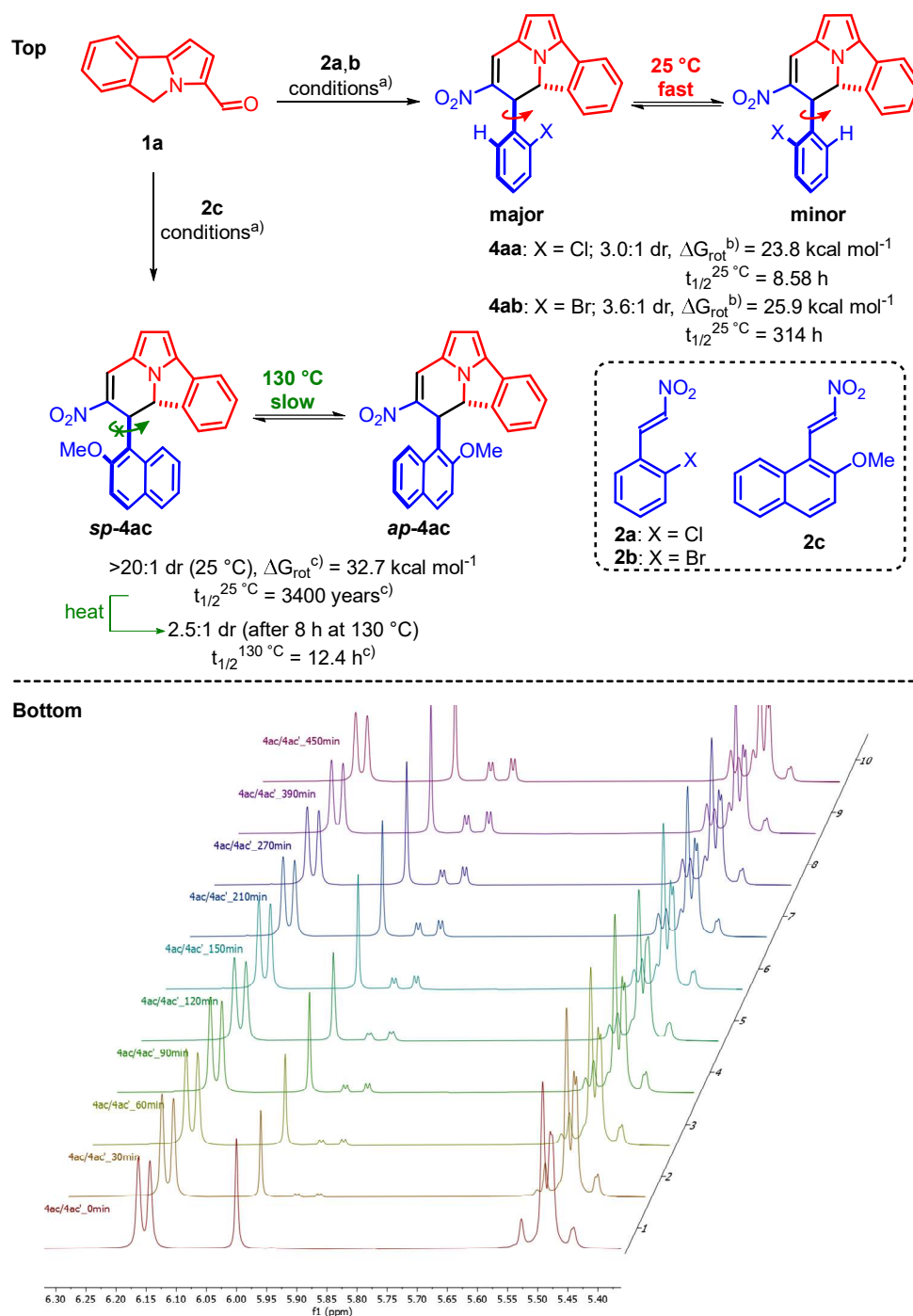
Figure 2. Substrate design. Top: preliminary investigation: search of substrate requirements. a) Reaction conditions: **1a** (0.05 mmol, 1 equiv.), **2** (0.06 mmol, 1.2 equiv.), pyrrolidine (0.02 mmol, 20 mol%), **3a** (2-MeBzOH, 0.04 mmol, 40 mol%), CDCl$_3$ (0.3 mL, 0.17 M), 60 °C, 18 h. b) Calculated at the ωB97X-D/Def2-TZVPP/SMD(CHCl$_3$) level of theory. c) Experimentally determined value (see Supporting Information). Bottom: Stacked ^{1}H NMR spectra (relevant region) showing appearance of *ap*-**4ac** over time. In order to designate the *sp* or *ap* descriptors, the priority is assigned to the carbons next to the one bearing

the stereogenic axis following the Cahn-Ingold-Prelog (CIP) rules. In this specific case, we consider the MeO-substituent of the naphthalene moiety and the carbon bearing the NO$_2$-substituent as the two groups with highest priority.

Initial tests applying the well-established catalysts **A**[40] or **B**,[41] failed to promote the desired reaction (Table 1). Instead, catalyst **C**[42] or **D**,[43] lacking one element of steric bulk on the α-substituent, were found to facilitate the asymmetric formation of *sp*-**4ac** with the simultaneous control of two stereogenic centers and a stable C(sp^2)–C(sp^3) stereogenic axis. As a general trend, we observed that the process shows lower values of enantioselectivities at higher levels of conversion (exemplified in Table 1 for catalyst **C** and acid **3a**, entries 1-3; see Supporting Information for other acid-catalyst combinations showing the same behavior). This identifies conditions in entry 4 as optimal to obtain highly enantioenriched *sp*-**4ac** with the highest possible efficiency. A screening of acids revealed that pivalic acid **3b** delivered the desired product with excellent enantioselectivity and comparable yield (see Supporting Information for further optimization).

Table 1. Representative Results from the Optimization of the Reaction Conditions (see Supporting Information).
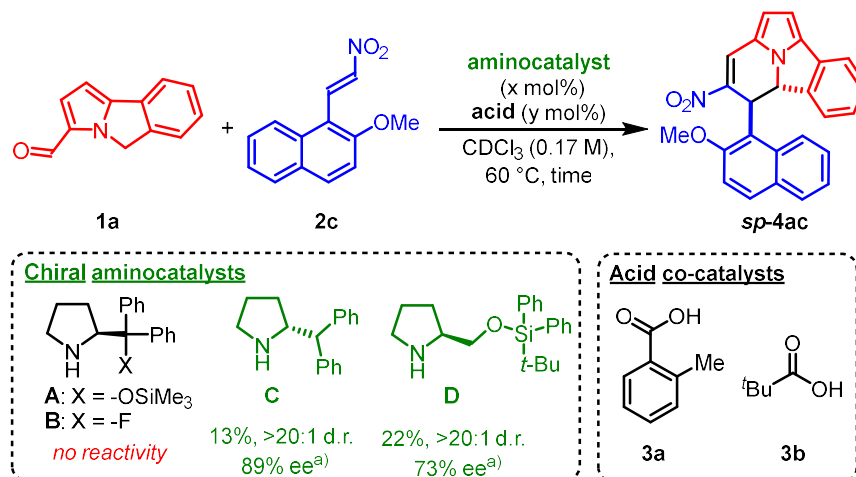
Entry[b]	Cat. (mol%)	Acid (mol%)	Yield (%) (time)	ee (%)	Yield (%) (time)	ee (%)
1	**C** (20)	**3a** (20)	15 (42 h)	89	23 (114 h)	78
2	**C** (20)	**3a** (40)	20 (42 h)	78	38 (114 h)	57
3	**C** (40)	**3a** (20)	36 (42 h)	88	54 (114 h)	75
4	**C** (40)	**3b** (20)	-	-	54 (90 h)	95

Scope of the reaction. Once the optimal reaction conditions were established, we evaluated the substrate scope (Table 2). The present methodology proved to be general for a variety of aldehydes **1** bearing substituents of a diverse nature either on the benzene or the pyrrole ring (*sp*-**4ac**-*sp*-**4hc** and *sp*-**4kc** 32-62% yield, >20:1 d.r. in all cases and >92% ee). Notably, aldehydes **1i** and **1j**, featuring additional steric hindrance in proximity of the reactive center, delivered, in the presence of catalyst **D**, the corresponding products *sp*-**4ic** and *sp*-**4jc** in excellent enantioselectivities and good yields. Nitroolefins **2** with different *O*-protecting groups, as well as various substituents on the naphthalene moiety, served for the smooth generation of an array of diverse atropisomeric cyclazines (*sp*-**4ad**-*sp*-**4ai**). Interestingly, the nature of the substituent at the 2-position of the naphthalene ring has a significant influence on the diastereoselectivity of the reaction, while the enantioselectivity remains unaffected. Whereas 2-bromo substituted nitroolefin **2j** delivered product *sp*,*ap*-**4aj** as an equimolar diastereomeric mixture, inversion of the conformation of the stereogenic axis, with moderate to excellent diastereoselectivity, was observed for *sp*-**4ak**, *sp*-**4al** and *ap*-**4am** compared to *sp*-**4ac**. In addition to this, we found that high levels of conformational stability of the C(sp^2)–C(sp^3) stereogenic axis could also be achieved in products *ap*-**4an**-*ap*-**4ap** possessing simple *ortho*-disubstituted phenyl rings; these were obtained as single diastereomers in good yields and excellent enantioselectivities (*vide infra*).

Atropisomeric systems featuring five-membered rings require higher degrees of demanding constraints to stabilize the stereogenic axis. The combination of these moieties with an intrinsically labile C(sp^2)–C(sp^3) stereogenic axis to form optically active atropisomers is an elusive goal.[44-46] Delightfully, product *ap*-**4aq** having a 2-methylbenzothiophene and *ap*-**4as** having a 2-*tert*-butylindole scaffolds show remarkable conformational stability at 60 °C and were indeed isolated in good diastereo- and enantioselectivity. On the other hand, product *ap*-**4ar**, featuring a protected 2-methylindole group, exhibited low enantioselectivity and slowly reached thermodynamic equilibration during the course of the reaction. Finally, the methodology was extended to different

electron-poor 2π-components, such as α-ketoesters **5** and α,β-unsaturated aldehydes **7**, the latter requiring slightly different reaction conditions (see Supporting Information). The corresponding products **6** and **8**, displaying the same level of conformational stability of products **4**, were obtained with excellent results, showing that the disclosed process is not limited to nitroolefins **2** as electrophiles (*vide infra*).

Absolute configuration was determined for product ***sp*-4fc** by single crystal X-ray analysis. All other relative configurations were assigned by analogy and supported by 2D NMR. In the case of product ***sp*-8a**, the absolute configuration was determined by comparison between calculated and experimental ECD spectra (see Supporting Information).

In order to demonstrate the conformational stability of these atropisomers, we measured the rotational barrier of a series of products, each one displaying different functionalities. As mentioned before, compound ***sp*-4ac** displayed a rotational barrier of 32.7 kcal mol^{-1}, $t_{1/2}^{25\,°C}$ = 3400 y; furthermore, product ***sp*-4ic**, featuring a methyl substituent in proximity of the stereogenic axis, has a comparable rotational barrier (ΔG^{rot} = 31.8 kcal mol^{-1}, $t_{1/2}^{25\,°C}$ = 697 y). Product ***ap*-4ap** featuring an *ortho*-disubstituted aryl moiety, instead of the naphthalene ring, showed an even higher value for the rotational barrier (ΔG^{rot} = 33.4 kcal mol^{-1}, $t_{1/2}^{25\,°C}$ = 11136 y). We were pleased to demonstrate that similar levels of conformational stability were obtained for products ***sp*-6a** (ΔG^{rot} = 33.2 kcal mol^{-1}, $t_{1/2}^{25\,°C}$ = 9894 y) and ***sp*-8a** (ΔG^{rot} = 31.7 kcal mol^{-1}, $t_{1/2}^{25\,°C}$ = 641 y) featuring a keto-ester or a hydroxymethyl moiety, respectively; the latter is obtained by reduction of the corresponding aldehyde.

Table 2. Scope of the Stereoselective Preparation of C(sp^2)–C(sp^3) Atropisomers for the Reaction Between Aldehydes **1** and Electron-deficient Olefins **2**, **5**, **7**.

$$1 + 2, \text{EWG} = NO_2;\ 5, \text{EWG} = C(O)CO_2Me;\ 7, \text{EWG} = CHO \xrightarrow[\substack{\text{CDCl}_3 (0.17\ M) \\ 60\,°C,\ 42\text{-}162\ h}]{\substack{\textbf{C or D} (40\ mol\%) \\ \textbf{3b} (20\ mol\%).\ 4\ \text{Å MS}}} 4, \text{EWG} = NO_2;\ 6, \text{EWG} = C(O)CO_2Me;\ 8, \text{EWG} = CHO\ (CH_2OH)$$

sp-4ac, R = H, 54%, >20:1 d.r., 96% ee
sp-4bc, R = 8-MeO, 47%, >20:1 d.r., 97% ee
sp-4cc, R = 8-CF₃, 32%, >20:1 d.r., 92% ee
sp-4dc, R = 8-CO₂Me, 33%, >20:1 d.r., 92% ee
sp-4ec, R = 8-ᵗBu, 62%. >20:1 d.r., 97% ee
sp-4fc, R = 8-Br, 52%, >20:1 d.r., 93% ee
sp-4gc, R = 7-CF₃, 34%, >20:1 d.r., 96% ee
sp-4hc, R = 7,9-(Me)₂, 42%, >20:1 d.r., 97% ee
sp-4icᵃ⁾, R = 6-Me, 54%, >20:1 d.r., 96% ee
sp-4jcᵃ⁾, R = 6,7-(CH)₄-, 45%, >20:1 d.r., 92% ee
sp-4kc, R = 1-Br, 52%, >20:1 d.r., 98% ee

sp-4ad, X = Ms, R = H, Y = CH, 57%, 10:1 d.r., 99% ee
sp-4ae, X = MOM, R = H, Y = CH, 61%, >20:1 d.r., 98% ee
sp-4af, X = Me, R = 6-Br, Y = CH, 53%, >20:1 d.r., 90% ee
sp-4ag, X = Me, R = 6-MeO, Y = CH, 47%, >20:1 d.r., 92% ee
sp-4ah, X = Me, R = 7-MeO, Y = CH, 42%, >20:1 d.r., 96% ee
sp-4ai, X = Me, R = H, Y = N, 68%. >20:1 d.r., 62% ee

sp,ap-4aj, X = Br, 34%, 1:1 d.r., 91%, 99% ee
sp-4akᵃ⁾, X = vinyl, 57%, 4:1 d.r., 92% ee
sp-4al, X = Me, 40%, 10:1 d.r., 99% ee
ap-4amᵃ⁾, X = Ph, 48%, >20:1 d.r., 96% ee

ap-4an, X = Cl, R =H, 59%, >20:1 d.r., 92% ee
sp-4ao, X= Me, R = OMe, 61%, >20:1 d.r., 98% ee
ap-4ap, X = Br, R = H, 61%, >20:1 d.r., 95% ee

ap-4aq, X = S, R = Me, 59%. 6:1 d.r., 84% ee
ap-4ar, X = NTs, R = Me 57%, 5:1 d.r., 33% ee
ap-4asᵃ⁾, X = NH, R = ᵗBu, 27%, 13:1 d.r., 97% ee

sp-6a, R = H, 69%, 10:1 d.r., 92% ee
sp-6e, R = 8-ᵗBu, 68%, >20:1 d.r., 87% ee
sp-6h, R = 7,9-(Me)₂, 43%, 15:1 d.r., 92% ee

sp-8aᵇ⁾, R = H, 62%, >20:1 d.r., 90% ee
sp-8eᵇ⁾, R = 8-ᵗBu, 54%, >20:1 d.r., 93% ee
sp-8gᵇ⁾, R = 7-CF₃, 63%, >20:1 d.r., 73% ee

Reaction conditions, unless otherwise noted: **1** (0.1 mmol, 1 equiv.), **2** or **5** (0.12 mmol, 1.2 equiv.), **C** (0.04 mmol, 40 mol%), **3b** (0.02 mmol, 20 mol%), CDCl₃ (0.6 mL, 0.17 M), 60 °C, 42-162 h (for specific reaction times see Supporting Information). The yield given is isolated yield after column chromatography; diastereomeric ratio (d.r.) is determined by ¹H NMR analysis of the crude mixture; enantiomeric excess (ee) is determined by chiral stationary phase UPCC. a) Catalyst **D** (0.04 mmol, 40 mol%) was used; the product has opposite absolute configuration. b) Reaction conditions: **1** (0.1 mmol, 1 equiv.), **7** (0.15 mmol, 1.5 equiv.), **D** (0.02 mmol, 20 mol%), *o*-F-BzOH (0.02 mmol, 20 mol%), CDCl₃ (0.6 mL, 0.17 M), 40 °C,

66 h. The product is isolated after $NaBH_4$ reduction. In some products, such as *sp*-**4ak** and *sp*-**4al**, the inversion of the conformation of the stereogenic axis is accompanied by the change in priority of the substituents.

Central-to-axial chirality conversion. The isolation of molecules exhibiting unique properties is fundamental to experimentally verify the theoretical paradigms of chemistry. For example, the unprecedented formation of enantioenriched $C(sp^2)$–$C(sp^3)$ atropisomers can be exploited to confirm the founding principle of *central-to-axial chirality conversion* which is at the root of many stereoselective syntheses of axially chiral compounds.[33-36,47,48] It is generally proposed that these processes rely on the formation of an enantioenriched intermediate possessing exclusive central chirality; then, this species undergoes a transformation (either spontaneous or induced) to the desired atropisomeric product, with conversion of chirality. Potentially, this step may proceed with erosion of the enantiomeric excess. To explain this, it is postulated that the aforementioned intermediate exists as two different rotamers, either one converting to the opposite mirror image of the axially chiral product. In order to prove this concept experimentally, the two "rotamers" must be subjected separately to the chirality conversion step. This requires the isolation of enantioenriched and conformationally stable $C(sp^2)$–$C(sp^3)$ atropisomers.

Compound *ap*-**4ac** (94% ee) was isolated and characterized upon thermal equilibration of enantioenriched *sp*-**4ac**, followed by chromatographic separation (Scheme 2). It should be noted that this process only involves the rotation around the $C(sp^2)$–$C(sp^3)$ axis, leaving the absolute configuration of its sp^3-stereogenic carbon unchanged. Then, rotamers *sp*-**4ac** and *ap*-**4ac** were separately oxidized to aromatic atropisomeric cyclazines **9** and **9-ent**, respectively, with complete retention of enantiomeric excess and starting conformation of the stereogenic axis (see Supporting Information). This result is the empirical evidence for the operating principle of *central-to-axial chirality conversions*.

Scheme 2. Oxidation of *sp*-**4ac** and *ap*-**4ac** into Enantiomeric Compounds **9** and **9-ent**.
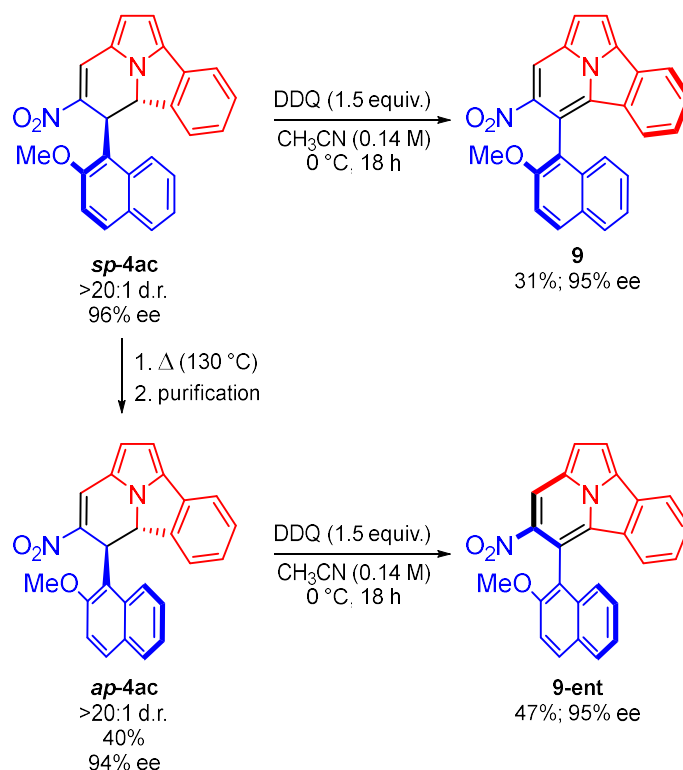
Computational studies. Interested in the origin of the observed selectivity, with a particular interest on the atropselectivity, we turned to DFT calculations to probe the reaction pathway. The entire system of 5*H*-benzo[*a*]pyrrolizine-3-carbaldehyde **1a** reacting with nitroolefin **2c**, catalyzed by organocatalyst **C** and acetic acid was modeled, as it has been observed to provide comparable results (see Supporting Information). Our proposed mechanism begins with the condensation of **1** with organocatalyst **C** to form the reactive intermediate **I** (Scheme 3). This intermediate then reacts with nitroolefin **2c** in **TS-CC** to establish the first carbon-carbon bond. The generated zwitterion **II** then closes the nitronate carbon onto the iminium carbon in **TS-ring** to form intermediate **III**. This intermediate then undergoes elimination (**TS-elim**) to alleviate product *sp*-**4ac** and facilitate catalyst turnover.

Scheme 3. Proposed Catalytic Cycle.

13
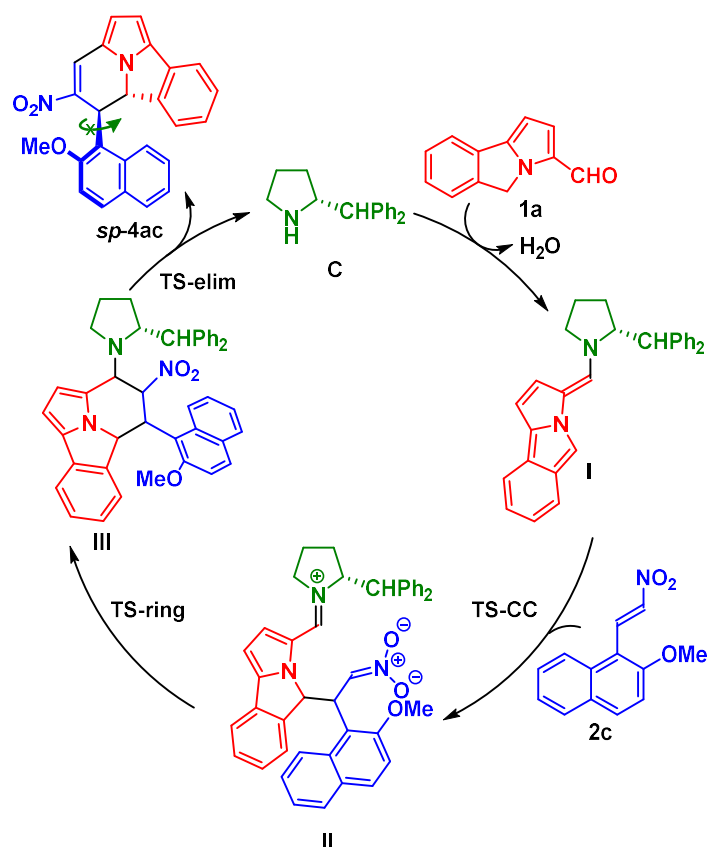
Investigation of the potential energy surface began with the systematic interrogation of **TS-CC** and **TS-ring** for all possible stereogenic outcomes (see Supporting Information). From this exploration, it became evident that the stereochemistry of the final product was dependent on **TS-elim**, implying the reversibility of the formation of C–C bond and the ring-closure step. Eliminations corresponding to E2, E1, and E1cB mechanisms were modeled and it was shown that the E1cB pathway was preferred for the formation of the major enantiomer **sp-4ac**, the minor enantiomer **sp-4ac-ent**, and the atropisomer **ap-4ac** (see Supporting Information).

The transition state leading to the minor enantiomer of product **TS-E1cB-1**$_{sp\text{-}4ac\text{-}ent}$ is calculated to be 3.2 kcal mol^{-1} higher in energy than that leading to the major enantiomer **TS-E1cB-1**$_{sp\text{-}4ac}$ (Figure 3). This leads to a predicted 98% ee, which is in good agreement with the observed value (96% ee).
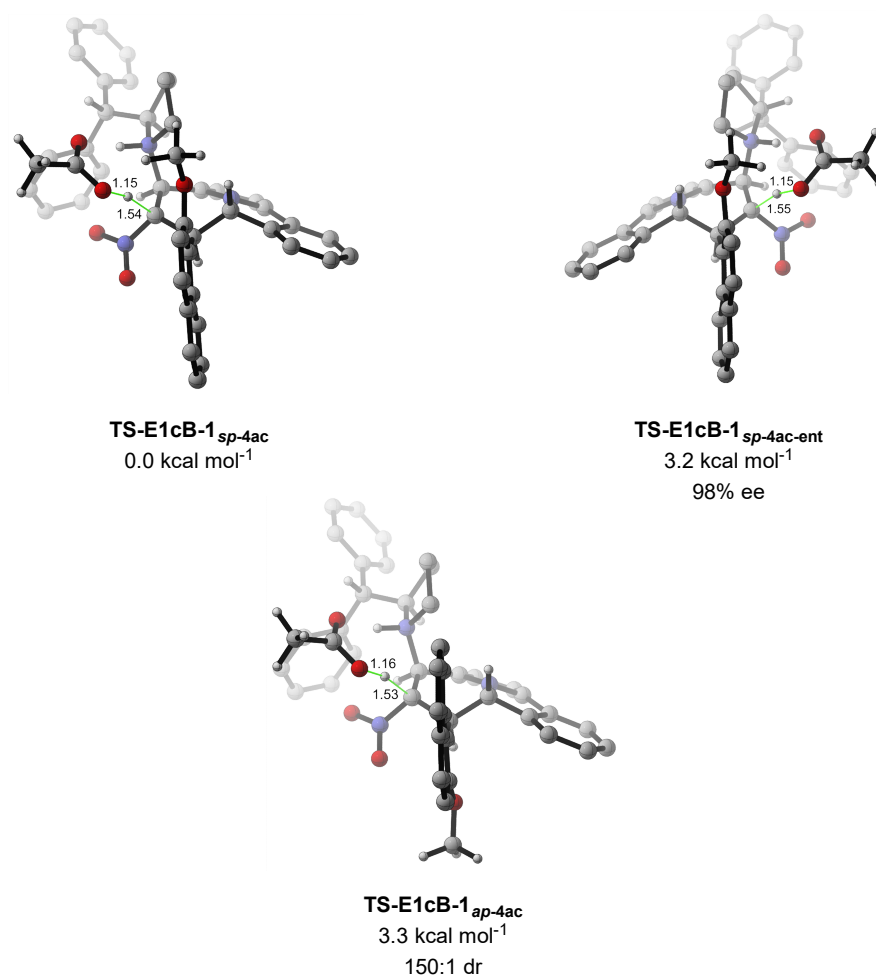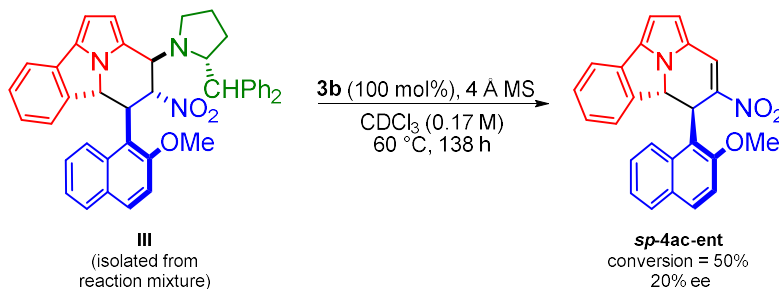
Figure 3. Transition state structures for **TS-E1cB-1** leading to *sp*-**4ac**, *sp*-**4ac-ent**, and *ap*-**4ac**, and Relative energies, some atoms not shown for clarity, distances in Ångstrøm.

Experimental investigation led to the isolation of an intermediate from the reaction mixture. NMR analysis identified the species as **III** (Scheme 4, see also Supporting Information), corroborating that catalyst elimination is the rate-determining step of the process. The intermediate (isolated as a mixture of diastereomers) was subjected to the reaction conditions delivering a 20% ee in favor of product *sp*-**4ac-ent**, suggesting partial reversibility of the formation of all stereocenters and the stereogenic axis, as well as accumulation of **III**$_{sp\text{-4ac-ent}}$, over **III**$_{sp\text{-4ac}}$, indicating a faster elimination of the latter.

Scheme 4. Isolated Intermediate **III** Subjected to the Reaction Conditions Providing *sp*-**4ac-ent** as Major Enantiomer of the Product.

III
(isolated from
reaction mixture)

3b (100 mol%), 4 Å MS
CDCl$_3$ (0.17 M)
60 °C, 138 h

sp-**4ac-ent**
conversion = 50%
20% ee

Surprisingly, it was calculated that the barrier of rotation for intermediate **III** is 35.1 kcal mol^{-1}, suggesting no equilibration between **III**$_{sp\text{-}4ac}$ and **III**$_{ap\text{-}4ac}$ (see Supporting Information). The atroposelectivity likely arises from a Curtin-Hammett scenario in which the two diastereomeric intermediates **III**$_{sp\text{-}4ac}$ and **III**$_{ap\text{-}4ac}$ are in equilibrium with each other and are connected by more than one transition state. Thus, **III**$_{ap\text{-}4ac}$ converts to **III**$_{sp\text{-}4ac}$ (and *vice versa*) through a retro-cycloaddition-cycloaddition sequence. A $\Delta\Delta G^{\ddagger}$ between **TS-E1cB-1**$_{sp\text{-}4ac}$ and **TS-E1cB-1**$_{ap\text{-}4ac}$ of 3.3 kcal mol^{-1} gives rise to a predicted diastereomeric ratio of ~150 to 1 which is again in good agreement with the observed diastereoselectivity (d.r. >20:1). These computational investigations lead us to suggest the energy profile in Figure 4.
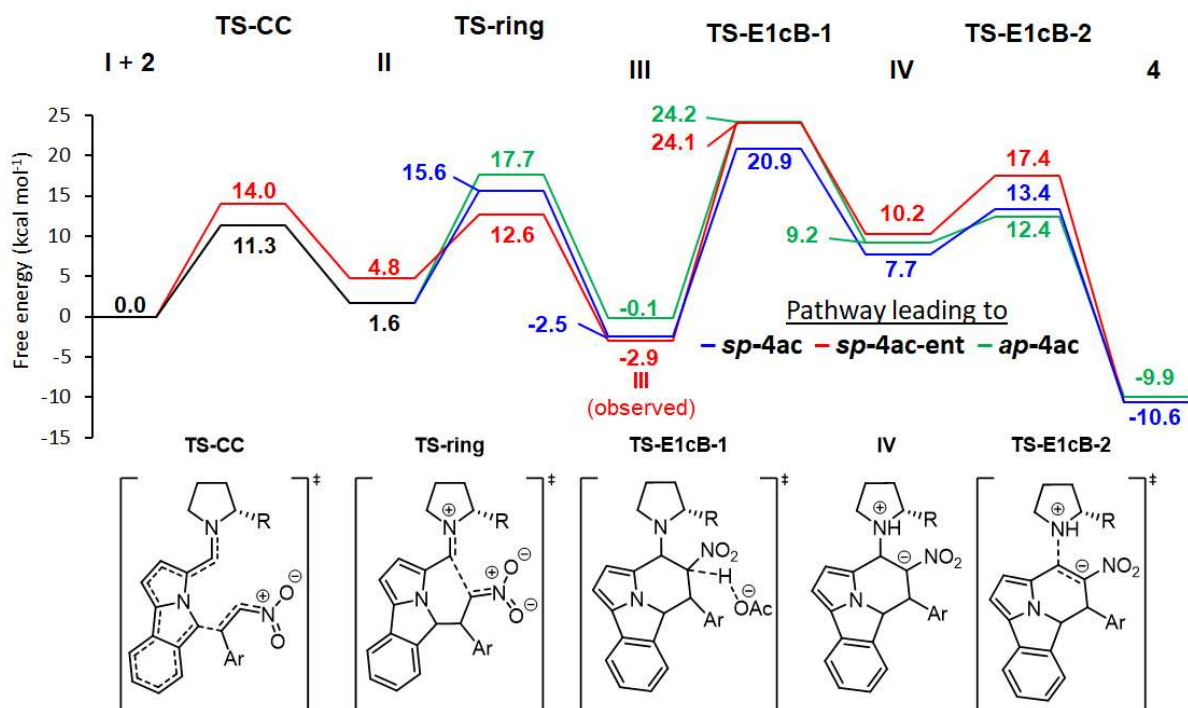
Figure 4. Free energy profile leading to products ***sp*-4ac**, ***sp*-4ac-ent**, and ***ap*-4ac**. Calculations performed at B3LYP-D3(BJ)/Def2-TZVPP/SMD(CHCl$_3$)//B3LYP/6-31G(d)/SMD(CHCl$_3$). Data calculated for Ar = 2-methoxy-1-naphthyl.

CONCLUSION

The first access to enantioenriched atropisomeric scaffolds exhibiting the simultaneous presence of a conformationally stable C(sp^2)–C(sp^3) stereogenic axis and a center of asymmetry has been developed. The present methodology showcases an enantioselective aminocatalytic cycloaddition between 5*H*-benzo[*a*]pyrrolizine-3-carbaldehydes and electron-poor olefins to obtain molecular frameworks based on the cycl[3.2.2]azine moiety. The reaction is shown to accommodate a wide variety of substrates, leading to the formation of diverse products that possess this unique stereogenic axis. The rotational barrier of the parent compound has been measured experimentally and both atropisomers have been isolated and characterized upon thermal equilibration. In addition, the evaluation of the conformational stability of compounds having different substitution patterns was carried out, showing half-life times >640 years. Importantly, the isolation of such unique compounds provided, through a simple oxidative transformation, the empirical evidence for the operating principle of central-to-axial chirality conversions. DFT-calculations, supported by the isolation of a reactive intermediate, showed how the stereoselectivity of the reaction is

17

controlled by the Curtin-Hammett principle, with a single transition state (the elimination step) dictating both the atropo- and the enantioinduction.

ASSOCIATED CONTENT

Supporting Information.

The Supporting Information is available free of charge at: http://pubs.acs.org. Experimental procedures, characterization data, NMR spectra, UPCC spectra, theoretical calculations (PDF), and X-ray crystallographic data for ***sp*-4fc** (CIF).

AUTHOR INFORMATION

Corresponding Author

*Karl Anker Jørgensen – *Department of Chemistry, Aarhus University, DK-8000 Aarhus C, Denmark;* orcid.org/0000-0002-3482-6236; Email: kaj@chem.au.dk

Authors

Giulio Bertuzzi − *Department of Chemistry, Aarhus University, DK-8000 Aarhus C, Denmark*
Vasco Corti − *Department of Chemistry, Aarhus University, DK-8000 Aarhus C, Denmark*
Joseph A. Izzo − *Department of Chemistry, Aarhus University, DK-8000 Aarhus C, Denmark*
Sebastijan Ričko − *Department of Chemistry, Aarhus University, DK-8000 Aarhus C, Denmark; Aarhus Institute of Advanced Studies (AIAS), Aarhus University, DK-8000 Aarhus C, Denmark*
Nicolaj Inunnguaq Jessen − *Department of Chemistry, Aarhus University, DK-8000 Aarhus C, Denmark*

Notes

The authors declare no competing financial interest.

ACKNOWLEDGMENT

REFERENCES

1. Bringmann, G.; Mortimer, A. J. P.; Keller, P. A.; Gresser, M. J.; Garner, J.; Breuning, M. Atroposelective Synthesis of Axially Chiral Biaryl Compounds. *Angew. Chem. Int. Ed.* **2005**, *44*, 5384.

2. Wencel-Delord, J.; Panossian, A.; Leroux, F. R.; Colobert, F. Recent Advances and New Concepts for the Synthesis of Axially Stereoenriched Biaryls. *Chem. Soc. Rev.* **2015**, *44*, 3418.

3. Gustafson, J. L.; Lim, D.; Miller, S. J., Dynamic Kinetic Resolution of Biaryl Atropisomers via Peptide-Catalyzed Asymmetric Bromination. *Science* **2010**, *328*, 1251.

4. Cheng, J. K.; Xiang, S.-H.; Li, S.; Ye, L.; Tan, B. Recent Advances in Catalytic Asymmetric Construction of Atropisomers. *Chem. Rev.* **2021**, *121*, 4805.

5. Noyori, R.; Takaya, H. BINAP: An Efficient Chiral Element for Asymmetric Catalysis. *Acc. Chem. Res.* **1990**, *23*, 345.

6. Kočovskŷ, P.; Vyskočil, Ŝ.; Smrčina, M. Non-Symmetrically Substituted 1,1'-Binaphthyls in Enantioselective Catalysis. *Chem. Rev.* **2003**, *103*, 3213.

7. Parmar, D.; Sugiono, E.; Raja, S.; Rueping, M. Complete Field Guide to Asymmetric BINOL-Phosphate Derived Brønsted Acid and Metal Catalysis: History and Classification by Mode of Activation; Brønsted Acidity, Hydrogen Bonding, Ion Pairing, and Metal Phosphates. *Chem. Rev.* **2014**, *114*, 9047.

8. Smyth, J. E.; Butler, N. M.; Keller, P. A. A Twist of Nature – the Significance of Atropisomers in Biological Systems. *Nat. Prod. Rep.* **2015**, *32*, 1562.

9. Clayden, J.; Moran, W. J.; Edwards, P. J.; LaPlante S. R. The Challenge of Atropisomerism in Drug Discovery. *Angew. Chem. Int. Ed.* **2009**, *48*, 6398.

10. MacQuarrie, S.; Thompson, M. P.; Blanc, A.; Mosey, N. J.; Lemieux, R. P.; Crudden, C. M. Chiral Periodic Mesoporous Organosilicates Based on Axially Chiral Monomers: Transmission of Chirality in the Solid State. *J. Am. Chem. Soc.* **2008**, *130*, 14099.

11. Li, Q.; Green, L.; Venkataraman, N.; Shiyanovskaya, I.; Khan, A.; Urbas, A.; Doane, J. W. Reversible Photoswitchable Axially Chiral Dopants with High Helical Twisting Power. *J. Am. Chem. Soc.* **2007**, *129*, 12908.

12. Reisberg, S. H.; Gao, Y.; Walker, A. S.; Helfrich, E. J. N.; Clardy, J.; Baran, P. S. Total Synthesis Reveals Atypical Atropisomerism in a Small-molecule Natural Product, Tryptorubin A. *Science* **2020**, *367*, 458.

13. Kumarasamy, E.; Raghunathan, R.; Sibi, M. P.; Sivaguru, J. Nonbiaryl and Heterobiaryl Atropisomers: Molecular Templates with Promise for Atropselective Chemical Transformations. *Chem. Rev.* **2015**, *115*, 11239.

14. Shirakawa, S.; Liu, K.; Maruoka, K. Catalytic Asymmetric Synthesis of Axially Chiral o-Iodoanilides by Phase-Transfer Catalyzed Alkylations. *J. Am. Chem. Soc.* **2012**, *134*, 916.

15. Barrett, K. T.; Metrano, A. J.; Rablen, P. R; Miller, S. J. Spontaneous Transfer of Chirality in an Atropisomerically Enriched Two-axis System. *Nature* **2014**, *509*, 71.

16. Jia, S.; Chen, Z.; Zhang, N.; Tan, Y.; Liu, Y.; Deng, J.; Yan, H. Organocatalytic Enantioselective Construction of Axially Chiral Sulfone-Containing Styrenes. *J. Am. Chem. Soc.* **2018**, *140*, 7056.

17. Zheng, S. C.; Wu, S.; Zhou, Q.; Chung, L. W.; Ye, L.; Tan, B. Organocatalytic Atroposelective Synthesis of Axially Chiral Styrenes. *Nat. Commun.* **2017**, *8*, 15238.

18. Betson, M. S.; Clayden, J.; Worrall, C. P.; Peace, S. Three Groups Good, Four Groups Bad? Atropisomerism in *ortho*-Substituted Diaryl Ethers. *Angew. Chem. Int. Ed.* **2006**, *45*, 5803.

19. Casarini, D.; Foresti, E.; Gasparrini, F.; Lunazzi, L.; Misiti, D.; Macciantelli, D.; Villani, C. Conformational Studies by Dynamic NMR. 50. Atropisomerism in Hindered Naphthyl Sulfoxides: Structure, Stereodynamics, and Chiral Resolution. *J. Org. Chem.* **1993**, *58*, 5674.

20. Clayden, J.; Senior, J.; Helliwell, M. Atropisomerism at C-S Bonds: Asymmetric Synthesis of Diaryl Sulfones by Dynamic Resolution Under Thermodynamic Control. *Angew. Chem. Int. Ed.* **2009**, *48*, 6270.

21. Li, S.-G.; Wang, Y.-T.; Zhang, Q.; Wang, K.-B.; Xue, J.-J., Li, D.-H.; Jing, Y.-K.;, Lin, B.; Hua, H.-M. Pegaharmols A–B, Axially Chiral β-Carboline-quinazoline Dimers from the Roots of Peganum Harmala. *Org. Lett.* **2020**, *22*, 7522.

22. Isaka, M.; Tanticharoen, M.; Kongsaeree, P.; Thebtaranonth, Y. Structures of Cordypyridones A−D, Antimalarial *N*-Hydroxy- and *N*-Methoxy-2-pyridones from the Insect Pathogenic Fungus Cordyceps Nipponica. *J. Org. Chem.* **2001**, *66*, 4803.

23. Jones, I. L.; Moore, F. K.; Chai, C. L. L. Total Synthesis of (±)-Cordypyridones A and B and Related Epimers. *Org. Lett.* **2009**, *11*, 5526.

24. Nugroho, A. E.; Hirasawa, Y.; Kawahara, N.; Goda, Y.; Awang, K.; Hadi, A. H. A.; Morita, H. Bisnicalaterine A, a Vobasine−Vobasine Bisindole Alkaloid from Hunteria Zeylanica. *J. Nat. Prod.* **2009***, 72,* 1502.

25. Ford, W. T.; Thompson, T. B.; Snoble, K. A. J.; Timko, J. M. Hindered Rotation in 9-Arylfluorenes. Resolutions of the Mechanistic Question. *J. Am. Chem. Soc.* **1975**, *97*, 95.

26. Ōki, M. *The Chemistry of Rotational Isomers* (Springer, 1993).

27. Nakamura, M.; Ōki, M. Restricted Rotation Involving the Tetrahedral Carbon. XV. Restricted Rotation about a Csp^3–Csp^2 Bond in 9-Aryltriptycene Derivatives. *Bull. Chem. Soc. Jpn.* **1975**, *48*, 2106.

28. Lomas, J. S.; Dubois, J.-E. Conformational Isomerism in *o*-Tolyldi-*tert*-butylcarbinol. *J. Org. Chem.* **1976**, *41*, 3033.

29. Wu, X.; Witzig, R. M.; Beaud, R.; Fischer, C.; Häussinger, D.; Sparr, C. Catalyst Control over Sixfold Stereogenicity. *Nat. Catal.* **2021**, *4*, 457.

30. Schmidt, T. A.; Sparr, C. Catalyst Control over Twofold and Higher-Order Stereogenicity by Atroposelective Arene Formation. *Acc. Chem. Res.* **2021**, *54*, 2764.

31. Oki, M. Isolation of Rotational Isomers and Developments Derived Therefrom. *Proc. Jpn. Acad., Ser. B* **2010**, *86*, 867.

32. Nguyen, T. T. Traceless point-to-axial chirality exchange in the atropselective synthesis of biaryls/heterobiaryls. *Org. Biomol. Chem.* **2019**, *17*, 6952.

33. Quinonero, O.; Jean, M.; Vanthuyne, N.; Roussel, C.; Bonne, D.; Constantieux, T.; Bressy, C.; Bugaut, X.; Rodriguez, J. Combining Organocatalysis with Central-to-Axial Chirality Conversion: Atroposelective Hantzsch-Type Synthesis of 4-Arylpyridines. *Angew. Chem. Int. Ed.* **2016**, *55*, 1401.

34. Raut, V. S.; Jean, M.; Vanthuyne, N.; Roussel, C.; Constantieux, T.; Bressy, C.; Bugaut, X.; Bonne, D.; Rodriguez J. Enantioselective Syntheses of Furan Atropisomers by an Oxidative Central-to-Axial Chirality Conversion Strategy. *J. Am. Chem. Soc.* **2017**, *139*, 2140.

35. He, X.-L.; Zhao, H.-R.; Song, X.; Jiang, B.; Du, W.; Chen, Y.-C. Asymmetric Barton−Zard Reaction To Access 3-Pyrrole-Containing Axially Chiral Skeletons. *ACS Catal.* **2019**, *9*, 4374.

36. Zheng, S.-C.; Wang, Q.; Zhu, J. Catalytic Kinetic Resolution by Enantioselective Aromatization: Conversion of Racemic Intermediates of the Barton–Zard Reaction into Enantioenriched 3-Arylpyrroles. *Angew. Chem. Int. Ed.* **2019**, *58*, 9215.

37. LaPlante, S. R.; Fader, L. D.; Fandrick, K. R., Fandrick, D. R.; Hucke, O.; Kemper, R.; Miller, S. P. F.; Edwards, P. J. Assessing Atropisomer Axial Chirality in Drug Discovery and Development. *J. Med. Chem.* **2011**, *54*, 7005.

38. Di Iorio, N.; Filippini, G.; Mazzanti, A.; Righi, P.; Bencivenni, G. Controlling the C(sp3)–C(sp2) Axial Conformation in the Enantioselective Friedel–Crafts-Type Alkylation of β-Naphthols with Inden-1-ones. *Org. Lett.* **2017**, *19*, 6692.

39. Jessen, N. I.; Bertuzzi, G.; Bura, M.; Skipper, M. L.; Jørgensen, K. A. Enantioselective Construction of the Cycl[3.2.2]azine Core via Organocatalytic [12+2] Cycloadditions. *J. Am. Chem. Soc.* **2021**, *143*, 6140.

40. Klier, L.; Tur, F.; Poulsen, P. H.; Jørgensen, K. A. Asymmetric Cycloaddition Reactions Catalysed by Diarylprolinol Silyl Ethers. *Chem. Soc. Rev.* **2017**, *46*, 1080.

41. Sparr, C.; Schweizer, W. B.; Senn, H. M.; Gilmour, R. The Fluorine-Iminium Ion Gauche Effect: Proof of Principle and Application to Asymmetric Organocatalysis. *Angew. Chem. Int. Ed.* **2009**, *121*, 3111.

42. Melchiorre, P.; Jørgensen, K. A. Direct Enantioselective Michael Addition of Aldehydes to Vinyl Ketones Catalyzed by Chiral Amines. *J. Org. Chem.* **2003**, *68*, 4151.

43. Gerasyuto, A. I.; Hsung, R. P.; Sydorenko, N.; Slafer, B. A Formal [3+3] Cycloaddition Reaction. 5. An Enantioselective Intramolecular Formal Aza-[3+3] Cycloaddition Reaction Promoted by Chiral Amine Salts. *J. Org. Chem.* **2005**, *70*, 4248.

44. Bonne, D.; Rodriguez, J. Enantioselective Syntheses of Atropisomers Featuring a Five-Membered Ring. *Chem. Commun.* **2017**, *53*, 12385.

45. Bonne, D.; Rodriguez, J. A Bird's Eye View of Atropisomers Featuring a Five-Membered Ring. *Eur. J. Org. Chem.* **2018**, 2417.

46. Li, T.-Z.; Liu, S.-J.; Tan, W.; Shi, F. Catalytic Asymmetric Construction of Axially Chiral Indole-Based Frameworks: An Emerging Area. *Chem. Eur. J.* **2020**, *26*, 15779.

47. Berson, J. A.; Brown, E. Studies on Dihydropyridines. III. An Absolute Asymmetric Synthesis and an Attempted Conversion of Carbon Atom Asymmetry to Biphenyl Asymmetry. *J. Am. Chem. Soc.* **1955**, *77*, 450.

48. Meyers, A. I.; Wettlaufer, D. G. The Complete Intramolecular Transfer of a Central Chiral Element to an Axial Chiral Element. Oxidation of (*S*)-4-Naphthyldihydroquinolines to (*S*)-4-Naphthylquinolines. *J. Am. Chem. Soc.* **1984**, *106*, 1135.

GRAPHICAL ABSTRACT

C(sp²)—C(sp³) Atropisomers

Examples of known compounds with
restricted rotation around a
C(sp²)—C(sp³) axis

asymmetric organocatalysis

✔ New class of C(sp²)—C(sp³) atropisomers
✔ Enantioenriched (up to 99% ee)
✔ Kinetic control (>20:1 dr)
✔ Stable stereogenic axis ($t_{1/2}^{25\,°C}$ >640 y)
✔ Proof for "central-to-axial chirality conversion"